NJC

PAPER

View Article Online
View Journal | View Issue

Cite this: *New J. Chem.*, 2019, **43**, 16968

A unique dual sensor for the detection of DCNP (nerve agent mimic) and Cd^{2+} in water†

Ayndrila Ghosh, ‡ Sujoy Das, ‡ Saurodeep Mandal and Prithidipa Sahoo *

Received 26th June 2019,
Accepted 10th October 2019

DOI: 10.1039/c9nj03327k

rsc.li/njc

Both DCNP (nerve gas Tabun mimic) and Cd^{2+} are extremely toxic to mankind. We have focused our research on quantitative estimation of DCNP and Cd^{2+} in given water samples. A carbazole–pyrrole conjugate **CPC** has been designed and synthesized which possesses a unique characteristic feature of detecting two hazardous analytes DCNP and Cd^{2+} by giving two different optical responses *i.e.* visual color changes and fluorescence "turn-on" respectively. The PET based chemosensor **CPC** produces a new compound **CPC-1** and a highly fluorescent **CPC–Cd^{2+}** complex upon addition of DCNP and Cd^{2+}, respectively. The detection limit of **CPC** for DCNP and Cd^{2+} has been estimated to be 7.75 nM and 0.27 μM, respectively, at pH 7.0. Quantum chemical calculations have been executed to demonstrate the electronic properties and the mechanism of the receptor–donor interactions. The concentrations of DCNP and Cd^{2+} ions in various water samples have been estimated with the help of standard absorbance and fluorescence curves.

Introduction

Toxicity, the word that interprets the degree of damage of an organism caused by a chemical substance or a particular mixture of substances, has been a very well-known concept to human civilization for many years. Effects of toxicants, whether it is chemical, physical or pathogens, are dose dependent; even pure water can act as a toxicant when taken in too high a dose by biological systems.[1] In the performing stage of chemical toxicants, nowadays, various analogues of organophosphate appear to be promising candidates as nerve agents. These nerve agents disrupt the function of the acetylcholinesterase enzyme which catalyzes the neurotransmitter, acetylcholine. This disruption results in an effective paralysis of muscles including the heart muscle and the muscles used for breathing[2] finally leading to death.[3,4] Among all the nerve agents *i.e.* G-series, V-series, carbamates, Novichok agents and insecticides, the G-series nerve gases – tabun (GA), sarin (GB), and soman (GD) – claim the most attention due to their usage as warfare agents.[5–9] From their debut at the terrorist attack in the Tokyo subway in 1995 to the recent blast on 4 April 2017 in Khan Shaykhun, a city of Syria, the fatal destructive power of nerve gases has been exhibited again and again.[10–13] This dreadful threat to mankind forced researchers to focus on the detection of these nerve agents. By satisfying the characteristics of a practical and real time sensing system, in recent years, chemosensors[14–22] have become superior to almost all conventional sensing methods. This is why, we have streamed our research in this field and designed a new chemosensing probe, carbazole–pyrrole conjugate (**CPC**), that not only can accomplish a selective, rapid naked eye detection of the tabun mimic – diethylcyanophosphonate (DCNP) – in the nanomolar range by forming a new compound **CPC-1** but also has been applied to quantify the DCNP concentration in various water samples (performance comparison Table S1, ESI†).

Surprisingly, it has been observed that when **CPC** detects the presence of DCNP by a colorimetric change from colorless to strong yellow, it is also able to give a vivid fluorescence "turn-on" response to the exposure of cadmium (Cd^{2+}) ions, a heavy metal toxicant. The vigorous use of cadmium in phosphate fertilizers, rechargeable nickel–cadmium batteries, silver–cadmium batteries, artists' colors, chalk pastels, smelting and refining of metals, electroplating, television phosphors, QLED TVs, semiconductors, photoconductors, quantum dots, control rods of nuclear reactors, the paint used on our house-hold crockeries, plastics and even in jewellery makes it important in agricultural and industrial areas respectively.[23–26] But this very same metal ion, *i.e.* Cd^{2+}, owing to a long half-life of 15–20 hours in the human body, can exert an extremely toxic effect through a strong bond formation with sulphur, resulting in the displacement of essential metal ions such as Zn^{2+} and Ca^{2+} from the binding sites of certain enzymes.[27–33] Cadmium is readily accumulated in the cells, kidneys, liver, lungs and stomach with ensuing physical disorders, *e.g.* headache, dizziness, chest pain, fever, pulmonary oedema, tracheo-bronchitis,

Department of Chemistry, Siksha Bhavana, Visva-Bharati University, Santiniketan, 731235, India. E-mail: prithidipa@hotmail.com

† Electronic supplementary information (ESI) available. See DOI: 10.1039/c9nj03327k

‡ These authors contributed equally to this work.

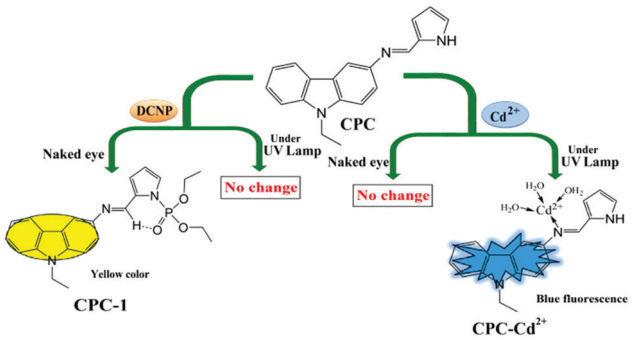

Scheme 1 Visual and fluorescence colour changes among **CPC**, **CPC-1** and the **CPC–Cd^{2+}** complex.

osteomalacia, proximal renal tubular dysfunction and carcinogenic effects.[34–38] According to the International Agency for Research on Cancer, the Environmental Protection Agency (EPA) and the European Chemical Agency, Cd^{2+} has been classified as a human carcinogen and the WHO (World Health Organization) has fixed the limit of Cd^{2+} to be 3 ppb in drinking water.[39–42] So, in the field of toxicology, cadmium(II) has attracted immense research interest.

Our probe **CPC** can selectively sense Cd^{2+} along with DCNP at the very same time both qualitatively and quantitatively (Scheme 1). **CPC** was synthesized with 70% yield through a simple one-pot reaction using just two reagents: 3-amino-9-ethylcarbazole and pyrrole-2-carboxaldehyde. The structure of the probe was deduced by ^{1}H NMR, ^{13}C NMR and mass spectral studies (Fig. S1–S3, ESI†).

Results and discussion

To establish the interactive properties of probe **CPC** towards its two target analytes *i.e.* DCNP and Cd^{2+}, a number of analytical and spectral techniques such as UV-vis, fluorescence, ^{1}H NMR, ^{13}C NMR, ^{31}P NMR titration studies and TD-DFT calculations have been exhaustively carried out and explained.

Spectral behaviour of CPC-1 with CPC

UV-vis titration has been performed in acetonitrile–water (1 : 6, v/v), buffered with 10 mM phosphate buffer (pH 7.0). The successive addition of 5 equiv. of DCNP (40, 80 and 100 μM) to **CPC** (20 μM) lowers the absorbance at 344 nm while at 417 nm the absorbance is increased significantly with a clear isosbestic point at 375 nm. This phenomenon is probably due to the attachment of a phosphonate group to probe **CPC** resulting in a new compound **CPC-1** which exhibits an intramolecular charge transfer (ICT) from the carbazole to pyrrole moiety (Fig. 1a). The formation of **CPC-1** from **CPC** is justified by its high association constant value (44.9×10^5 M^{-1}) (Fig. S4, ESI†). The detection limit of **CPC** for DCNP is 7.75 nM (Fig. S5, ESI†) where the standard curve is in the concentration range of 0–0.06 μM. Job's plot analysis reveals a 1 : 1 interaction stoichiometry between **CPC** and DCNP (Fig. S6, ESI†). The product, **CPC-1,** is quite stable in a wide range of pH from pH 6 to pH 14 though an acidic environment disturbs the

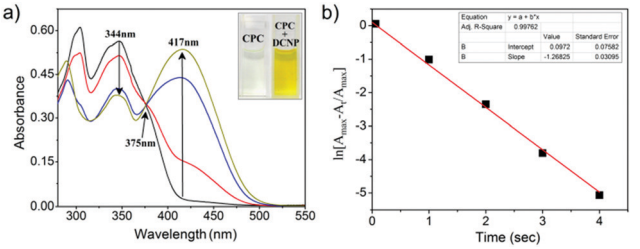

Fig. 1 (a) UV-vis absorption spectra of **CPC** (20 μM) in acetonitrile–water (1 : 6, v/v) and 10 mM phosphate buffer (pH 7.0), upon addition of **DCNP**. (b) Pseudo first-order kinetics plot for the reaction of **CPC** with DCNP.

stability (Fig. S7, ESI†). A time dependent absorbance intensity graph shows the formation of **CPC-1** from **CPC** within 5 seconds (Fig. S8, ESI†). The pseudo-first-order rate constant (k') has been calculated to be $k' = 1.26$ s^{-1} (Fig. 1b) according to eqn (1):

$$\ln[(A_{max} - A_t)/A_{max}] = -k't \quad (1)$$

where A_t and A_{max} are the absorbance at 417 nm at time 't' and the maximum value obtained after the reaction is complete, respectively, and k' is the observed pseudo-first order rate constant.

Spectral behaviour of CPC–Cd^{2+} with CPC

The absorbance study of **CPC** with Cd^{2+} showed a gradual decrease in absorbance at 304 and 344 nm (Fig. 2a) due to the termination of photoinduced electron transfer (PET) from the relatively high energy non-bonding electron pair on the pyrrole nitrogen to the fluorophore – the carbazole moiety. Here, the absorbance plot signifies a different mode of attachment between **CPC** and the cadmium(II) ion from that of DCNP. Fluorimetric titration reveals 17-fold hike in fluorescence intensity at 435 nm (λ_{ex} = 380 nm) after sequential addition of Cd^{2+} solution (up to 5 equiv.) to a 20 μM probe solution (Fig. 2b). Probably a non-covalent interaction between the cadmium ion and the imine nitrogen in **CPC** initiates a chelation enhanced fluorescence (CHEF) effect and the non-fluorescent probe exhibits a strong blue "turn-on" fluorescence response.

The binding affinity of the **CPC** probe towards Cd^{2+} has been measured through linear regression analysis and the value is 2.83×10^4 M^{-1} (Fig. S9, ESI†). From the detection limit calculation taking the linear range of 0–3.5 μM, it was found that **CPC**

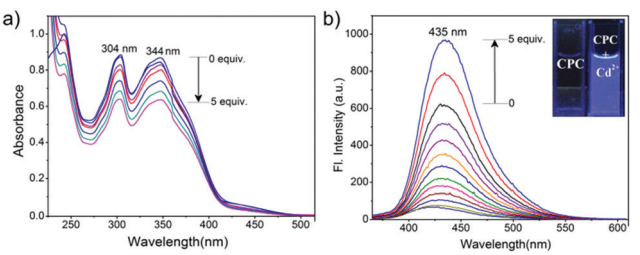

Fig. 2 (a) UV-vis absorption spectra of **CPC** (20 μM) in acetonitrile–water (1 : 6, v/v) and 10 mM phosphate buffer (pH 7.0), upon addition of Cd^{2+}. (b) Fluorescence emission spectra (λ_{ex} = 380 nm) of **CPC** (20 μM) in acetonitrile–water (1 : 6, v/v), neutral pH, with 5 equiv. of **Cd^{2+}**.

can detect Cd^{2+} at the limit concentration of 0.27 μM (Fig. S10, ESI†). The plot of fluorescence intensity as a function of different host/guest ratios shows a stoichiometric ratio of 1 : 1 for the **CPC–Cd^{2+}** complexation (Fig. S11, ESI†) and a plot of fluorescence intensity as a function of time confirms that a maximum of 30 seconds are required to complete this complexation (Fig. S12, ESI†). As the **CPC–Cd^{2+}** complex is base sensitive (Fig. S13, ESI†), all the spectral studies were performed in a buffered solution of pH 7.0.

Selectivity of CPC

When the selectivity of **CPC** was tested, the colorimetric observation clarified that only the addition of DCNP to the probe could give the strong yellow coloration from the colorless solution of **CPC** whereas other nerve agent simulants, ROS, RNS, gasotransmitters and metal cations (Fe^{2+}, Cu^{2+}, Zn^{2+}, Cd^{2+}, Pb^{2+}, Ni^{2+}, Ag^{2+}, Hg^{2+}, As^{3+}, Mg^{2+} and Ca^{2+}) including cadmium ions failed to do that. Interestingly, under a UV lamp the fluorescence turn on response of **CPC–Cd^{2+}** has been observed while the above said guests do not interfere the inherent non-fluorescent character of **CPC** (Fig. 3).

These practical observations have also been long-established from the comparative absorbance and fluorescence studies done with the above mentioned analyte solutions (Fig. 4).

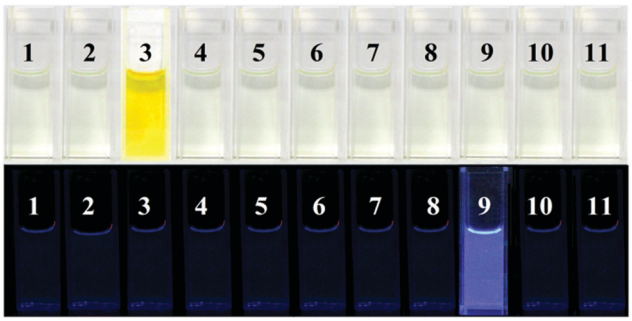

Fig. 3 Naked eye and fluorescence response of **CPC** (20 μM) to various guest molecules (100 μM). From left to right: (1) only **CPC**, **CPC** with (2) DCP, (3) DCNP, (4) NO, (5) CO, (6) H_2S, (7) Fe^{2+}, (8) Cu^{2+}, (9) Cd^{2+}, (10) Zn^{2+} and (11) Hg^{2+} in acetonitrile–water (1 : 6 v/v, pH 7.0, 10 mM phosphate buffer) solution.

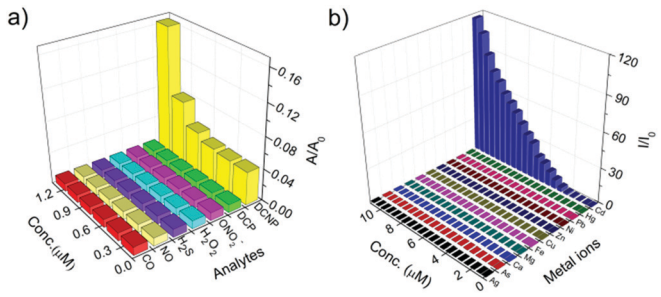

Fig. 4 (a) Comparative absorbance diagram of **CPC** with various nerve agent mimics, ROS, RNS and gasotransmitters added into acetonitrile–water (1 : 6, v/v) and 10 mM phosphate buffer (pH 7.0). (b) Comparative fluorescence diagram of **CPC** with different metal ions in acetonitrile–water (1 : 6, v/v) and 10 mM phosphate buffer (pH 7.0).

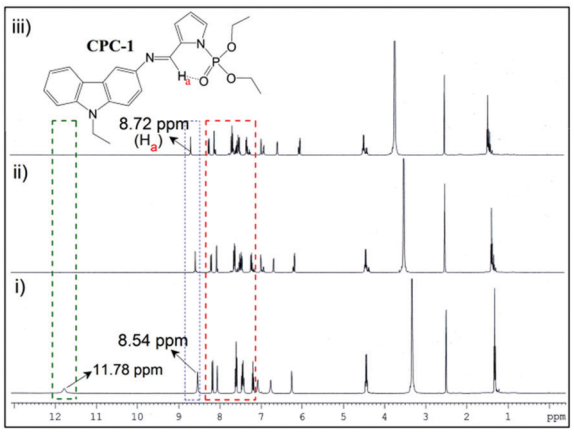

Fig. 5 Partial ^{1}H NMR titration [400 MHz] of **CPC** in DMSO-d_6 at 25 °C and the corresponding changes after the gradual addition of one equiv. of DCNP in D_2O from (i) only **CPC**, (ii) **CPC** + 0.5 equiv. of DCNP, (iii) **CPC** + 1 equiv. of DCNP.

NMR titration

NMR titration studies have been done to elucidate the interactions of **CPC** with DCNP and Cd^{2+}. In ^{1}H NMR titration, the disappearance of the characteristic proton peak of the –NH functional group in the pyrrole moiety at δ 11.78 ppm after addition of 1 equiv. of DCNP in the probe solution justifies the formation of the new compound, **CPC-1**. A downfield shift of carbazole protons indicate the electron transition from the carbazole to pyrrole moiety due to the formation of **CPC-1** where the phosphonate of DCNP abstracts electrons from carbazole through pyrrole nitrogen of **CPC** (Fig. 5). The gradual shift of the imine proton (H_a) from 8.54 ppm to 8.72 ppm and the proton–carbon coupling acquired from HMQC spectra of both **CPC** and **CPC-1** also corroborate the above electronic transition (Fig. S14 and S15, ESI†).

From further study of ^{31}P NMR titration, the appearance of a new peak at δ −13.42 ppm also confirms the formation of the new compound (Fig. 6).

On the other hand, in the **CPC–Cd^{2+}** complex, upon gradual addition of 1 equiv. of Cd^{2+} to **CPC**, there is a downfield shift of the pyrrole-NH_b of about 0.17 ppm (Fig. 7) and the aromatic protons of both carbazole and pyrrole have also shifted downfield which indicates the chelation of the Cd(II) with the probe, **CPC**. Here, we also observe the gradual downfield shift of imine proton H_c, evidencing the strong chelation in the **CPC–Cd^{2+}** complex.

Mass spectral titration studies

Partial mass (HRMS) spectra have also been recorded for the reaction mixtures of **CPC** with both DCNP and Cd^{2+} which give new peaks at *m*/*z*: 423.17 and at *m*/*z*: 455.07 specifying the formation of **CPC-1** and **CPC–Cd^{2+}**, respectively (Fig. S16 and S17, ESI†). These spectra also verify the 1 : 1 stoichiometric interaction between the probe and the analytes.

Theoretical analysis

Ground state optimization of the structures and the time dependent density functional theory (TDDFT) calculations for

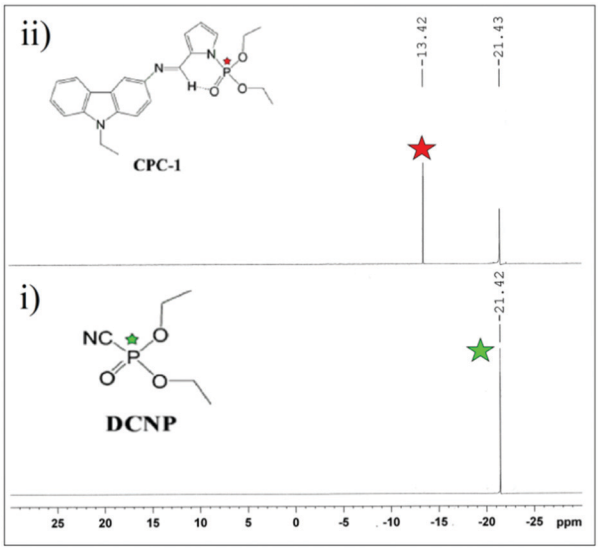

Fig. 6 ^{31}P NMR titration [400 MHz] of (i) DCNP and (ii) **CPC-1** in DMSO-d_6 at 25 °C showing the corresponding changes after formation of the new product.

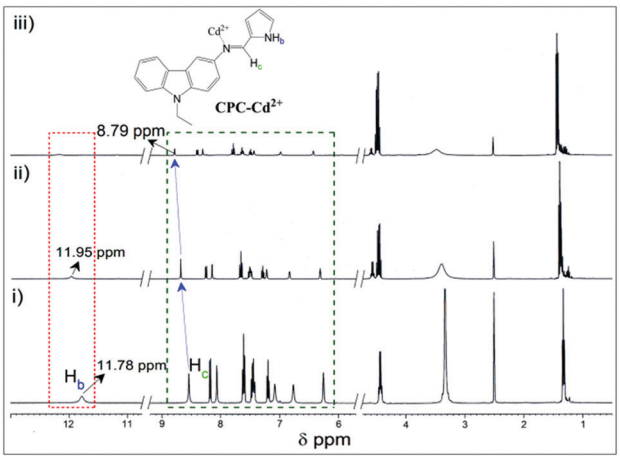

Fig. 7 Partial ^{1}H NMR titration [400 MHz] of **CPC** in DMSO-d_6 at 25 °C and the corresponding changes after the gradual addition of one equiv. of Cd^{2+} from (i) only **CPC**, (ii) **CPC** + 0.5 equiv. of Cd^{2+}, (iii) **CPC** + 1 equiv. of Cd^{2+}.

the probe with both products, *i.e.* **CPC-1** and the **CPC–Cd^{2+}** complex, have been studied using the hybrid exchange–correlation B3LYP functional (Becke, three parameter, Lee–Yang–Parr) and 6-311G** basis set implemented in the Gaussian 09 program (Fig. S18, ESI†).[43] The CPCM (Conductor like Polarizable Continuum Model) solvent model was used for solvent (H_2O) effect incorporation. In Tables S2–S4 (ESI†), all the energies of the optimized structures, vertical electronic transitions, *i.e.*, the calculated λ_{max}, orbital transition and oscillator strength (f) are listed.

Although a *cis–trans* free rotation is possible in probe **CPC**, theoretical calculation shows that the *trans*-isomer is more favourable with about 3.64 kcal mol^{-1} lower energy compared to the *cis*-isomer (Fig. 8 and Table S2, ESI†). The major transition in **CPC** at 366 nm ($S_0 \rightarrow S_1, f = 0.8193$) is very close to that observed at 344 nm experimentally. After addition of DCNP, the new absorbance peak observed at 390 nm ($S_0 \rightarrow S_1, f = 0.8338$)

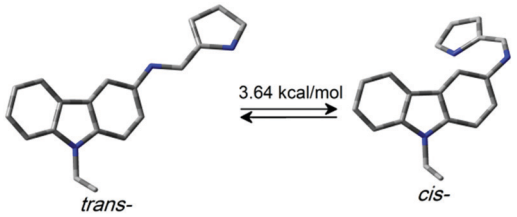

Fig. 8 Optimized structures of the *trans*- and *cis*-isomer of **CPC**.

resembles the enhanced absorbance at 417 nm obtained experimentally.

On complexation with Cd^{2+}, a sharp electronic transition ($f = 0.5608$) from the S_0 to the S_2 state has occurred at 403 nm which is comparable to the excitation wavelength for the fluorimetric titration *i.e.* 380 nm. The HOMO–LUMO energy gap of **CPC** is higher than that of the **CPC-1** and **CPC–Cd^{2+}** complex by 0.20 eV and 0.28 eV of energy respectively (Fig. 9). This theoretical study connects all the experimental findings.

Plausible mechanism and explanation

All the theoretical and experimental findings directed us to propose a schematic pathway by which probe **CPC** can detect DCNP and Cd^{2+} at the same time (Scheme 2). In the case of DCNP, the lone pair on pyrrole nitrogen attacks the phosphorous centre of DCNP, forcing the adjacent cyanide group to leave with the subsequent formation of **CPC-1** *via* deprotonation (Scheme S1, ESI†). The occurrence of PET from pyrrole to carbazole in **CPC** quenches the fluorescence of carbazole and makes the probe colorless but in the newly formed **CPC-1**, the presence of the electron withdrawing phosphonate group initiates the electron flow from the carbazole to pyrrole moiety thus leading to an intramolecular charge transfer (ICT) and develops the characteristic yellow colour of **CPC-1**.

In contrast, chelation of Cd^{2+} with **CPC** increases the rigidity of the complex **CPC–Cd^{2+}** by restricting the free rotation of the probe. Consequently, PET is terminated and the **CPC–Cd^{2+}** complex becomes highly fluorescent through the initiation of the CHEF effect. So, it is obvious that different modes of binding of these two analytes with **CPC** are the key reason for attainment of two different optical signals (Scheme 2).

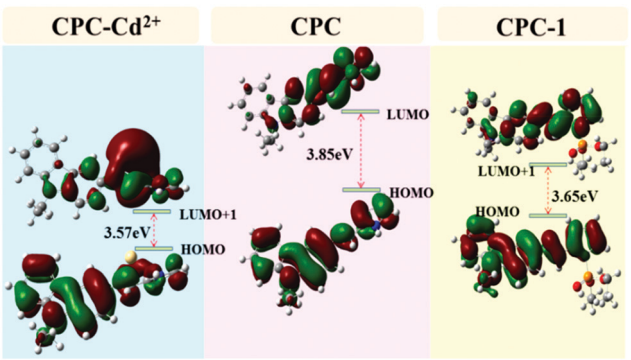

Fig. 9 Orbital distributions of the HOMO and LUMO in **CPC**, **CPC-1** and the **CPC–Cd^{2+}** complex.

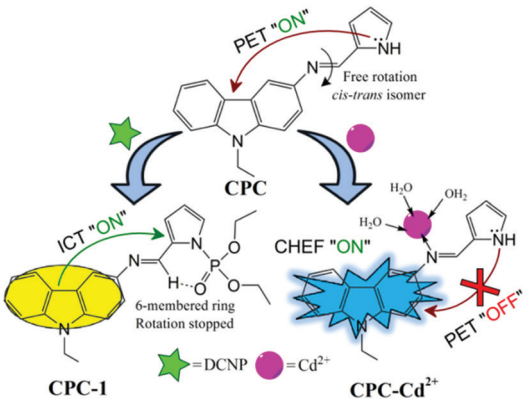

Scheme 2 Proposed scheme for simultaneous detection of DCNP and Cd^{2+} by **CPC**.

Quantitative analysis

To evaluate the quantification ability and the practical utility of our probe **CPC**, various water samples, *e.g.*, stagnant water, ground water and marine water, were used, as water is the most accumulated and important liquid in biosystems. Water bodies are the ultimate dumping station of all wastes or toxic materials. In fact, toxicants dumped in soil can contaminate the ground water of that particular area. We took tap water and pond water from Santiniketan, India, and sea water from Haldia Port area, Midnapore, India, for this quantitative study. 10, 15 and 20 nM of DCNP was added in each sample of volume 2 mL and absorbance changes were measured. The DCNP concentration was calculated using the standard curve of absorbance titration studies (Fig. 10). For all the samples the analyte recoveries were greater than 90% (Table 1 and Fig. S19, ESI†).

Surprisingly it was noticed that for all the samples, recoveries of Cd^{2+} calculated were greater than 100%. This finding confirmed the presence of the heavy metal toxicant, Cd^{2+}, in water of the areas from where the water samples were taken (Table 2 and Fig. S20, ESI†).

Vapour phase detection

CPC has high ability to detect DCNP not only in the solution phase but also in the vapour phase. We executed the detection experiment of DCNP in the vapour phase using our probe by a dip stick method. The experiment was conducted with the help of a cellulose paper strip which we had soaked in the probe solution and dangled in a stoppered conical flask containing DCNP solution in it.§ After 5 minutes it was observed that the colorless paper strip became yellow in color declaring the strong binding affinity of **CPC** to DCNP even in its vapour phase (Fig. 11).

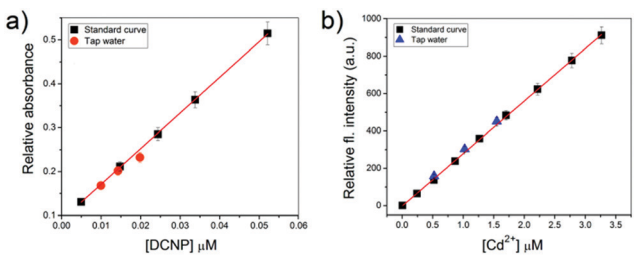

Fig. 10 Estimation of concentration of DCNP and Cd^{2+} in tap water samples using the standard graph. All the values are an average of three replicate measurements with standard deviation.

Table 1 Determination of DCNP in water samples

Sample	Added (nM)	Found (nM)	Recovery (%)
Ground water (tap water)	10	9.95	99.5
	15	14.27	95.1
	20	19.84	99.2
Stagnant water (pond water)	10	9.41	94.1
	15	14.35	95.6
	20	19.09	95.4
Marine water (sea water)	10	9.09	90.9
	15	13.99	93.2
	20	19.00	95.0

Table 2 Determination of Cd^{2+} in water samples

Sample	Added (μM)	Found (μM)	Recovery (%)
Ground water (tap water)	0.5	0.515	103.0
	1.0	1.030	103.0
	1.5	1.530	102.0
Stagnant water (pond water)	0.5	0.555	111.0
	1.0	1.090	109.0
	1.5	1.620	108.0
Marine water (sea water)	0.5	0.510	102.0
	1.0	1.04	104.0
	1.5	1.530	102.0

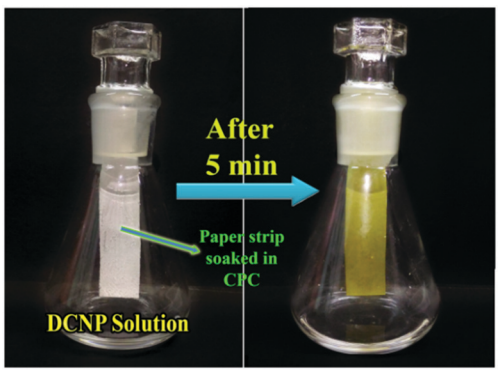

Fig. 11 Vapour phase detection of DCNP by **CPC**.

§ All the experiments done with DCNP were carried out in a sealed tube or a stoppered conical flask because of the toxic by-product HCN produced during the formation of the **CPC-1** compound. The solution in the reaction vessel was diluted 100 times by adding water and then treated with sodium hypochlorite solution (bleach) while the pH was maintained at greater than 10.0. The mixture was monitored with the help of a potassium iodide paper strip by checking whether it turned dark blue. If it turned, this confirmed the presence of excess bleach which converted the amenable cyanide to much less toxic cyanate ions (–CNO). These cyanate ions cannot reconvert to cyanide and moreover these will be dissociated into ammonia and carbon dioxide by certain bacteria present in soil. ^{1}H NMR, ^{13}C NMR, and MS spectra, additional spectroscopic data, supplementary fluorescence images, and theoretical calculation tables are given in the ESI.†

Experimental section

Materials and instruments

3-Amino-9-ethyl carbazole, pyrrole-2-carboxaldehyde, cadmium, iron, copper, mercury (all as metal perchlorate salts), diethylcyanophosphonate, and diethyl chlorophosphate were purchased from Sigma-Aldrich Pvt. Ltd (India). Materials were obtained from commercial suppliers and were used without further purification. Solvents were dried maintaining the conditions of standard procedures. Water used in all respective experiments was double distilled water. ^{1}H, ^{13}C and ^{31}P NMR spectra were recorded on a Bruker 400 MHz instrument. For NMR spectra and for NMR titration DMSO-d_6, D_2O were used as the solvent using trimethylsilane as an internal standard. Chemical shifts are expressed in δ ppm units and ^{1}H–^{1}H and ^{1}H–C coupling constants in Hz. The following abbreviations are used to describe spin multiplicities in ^{1}H NMR spectra: s = singlet; d = doublet; t = triplet; m = multiplet. The mass spectrum (HRMS) was recorded on a micromass Q-TOF Micro™ instrument using acetonitrile as a solvent. Fluorescence spectra were recorded on a PerkinElmer Model LS55 spectrophotometer. UV spectra were recorded on a SHIMADZU UV-3101PC spectrophotometer. Elemental analysis of the compounds was carried out on a PerkinElmer 2400 series CHNS/O Analyzer.

Synthesis of CPC

3-Amino-9-ethyl carbazole (0.42 g, 2 mmol) was dissolved in MeOH (15 mL). Pyrrole-2-carboxaldehyde (0.19 g, 2 mmol) was added to the solution and set to reflux for 12 hours (Scheme 3). The solvent was removed by evaporation. Water (20 mL) was added to the resultant mixture and extracted with $CHCl_3$ (20 mL × 2). The combined organic phase was washed twice with water, treated with brine and dried over Na_2SO_4. The product was purified through column chromatography using chloroform and ethyl acetate in 15 : 1 ratio as the eluent. After solvent evaporation under reduced pressure, a chocolate brown coloured solid product was obtained (0.40 g, 70% yield). ^{1}H NMR (400 MHz, DMSO-d_6): δ (ppm) = 11.78 (s, 1H), 8.54 (s, 1H), 8.186–8.167 (d, J = 7.6 Hz, 1H), 8.060 (s, 1H), 7.622–7.583 (t, J = 15.6 Hz, 2H), 7.472–7.413 (m, J = 23.6 Hz, 2H), 7.210–7.172 (t, J = 15.2 Hz, 1H), 7.077 (s, 1H), 6.763 (s, 1H), 6.248 (s, 1H), 4.468–4.416 (m, J = 20.8 Hz, 2H), 1.339–1.303 (t, J = 14.4 Hz, 3H). ^{13}C NMR (400 MHz, $CDCl_3$): δ (ppm) = 148.91, 140.56, 126.35, 123.26, 122.76, 121.02, 120.39, 119.11, 111.94, 110.41, 109.96, 109.68, 40.62, 40.42, 39.79, 39.58, 39.37, 37.53, 14.20. HRMS: anal. calcd for $C_{19}H_{17}N_3$: 287.14; found: 287.14 (M + H^+, 100%). Anal. calcd for$C_{19}H_{17}N_3$: C, 79.41; H, 5.96; N, 14.62; O, 9.57; found: C, 79.39; H, 5.92; N, 14.39.

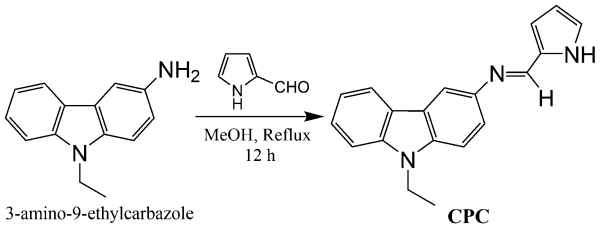

Scheme 3 Synthesis of the **CPC probe**.

Conclusion

To summarize, we have successfully developed a unique PET based chemosensor, **CPC**, which can easily and rapidly detect two deadly toxic analytes, *e.g.* DCNP which is a nerve agent mimic and widely used metal toxicant Cd^{2+}, at the very same time by showing different optical signals, *i.e.* visual changes for DCNP and fluorescence turn on for Cd^{2+}. The ability of estimation of guest concentrations even in the nano-molar range in water samples makes **CPC** efficient as a simple, less time consuming and cost-effective practical sensing system to estimate DCNP and Cd^{2+} in *in vitro* and *in vivo* samples. In addition, **CPC** could also be used as a potential tool to detect the presence of the nerve gas mimic DCNP in the vapour phase.

Conflicts of interest

There are no conflicts to declare.

Acknowledgements

PS acknowledges UGC, India, for awarding her a start-up grant [Project file no. F.30-7/2014 (BSR)]. AG and SD are sincerely thankful to UGC and CSIR, India, respectively, for research fellowships.

References

1 V. Dixit, *Toxicol. Res.*, 2019, **8**, 157–171.
2 F. R. Sidell, *Walter Reed Army Medical Center*, Borden Institute, 1997, ISBN 978-9997320919.
3 L. M. Eubanks, T. J. Dickerson and K. D. Janda, *Chem. Soc. Rev.*, 2007, **36**, 458–470.
4 A. W. Abu-Qare and M. B. Abou-Donia, *Food Chem. Toxicol.*, 2002, **40**, 1327–1333.
5 US Army, *FM 3–8 Chemical Reference handbook*, 1967.
6 D. H. Ellison, *Handbook of chemical and biological warfare agents*, CRC Press, Boca Raton, 2nd edn, 2007, ISBN 978-0-8493-1434-6. OCLC 82473582.
7 ''U.S. Army Destroys Entire Stockpile of VX Spray Tanks'' Archived 2009-02-06 at the Wayback Machine, U.S. Army Chemical Materials Agency, December 26, 2007, accessed January 4, 2007.
8 G. Vásárhelyi and L. Földi, *Acad. Appl. Res. Mil. Sci.*, 2007, **6**, 135–146.
9 N. A. Buckley, D. Roberts and M. Eddleston, *BMJ*, 2004, **329**, 1231–1233.
10 E. Croddy, *Jane's Intelligence Rev.*, 1995, **7**, 520–527.
11 N. Masuda, M. Takatsu, H. Morinari and T. Ozawa, *Lancet*, 1995, **345**, 1446–1447.
12 A. P. Volans, *J. Accid. Emerg. Med.*, 1996, **13**, 202–206.

13 ''Chemical attack of 4 April 2017 (Khan Sheikhoun): Clandestine Syrian chemical weapons programme''. Retrieved 2017-04-26.
14 L. Chen, D. Wu and J. Yoon, *ACS Sens.*, 2018, **3**, 27–43.
15 G. Yue, S. Su, N. Li, M. Shuai, X. Lai, D. Astruc and P. Zhao, *Coord. Chem. Rev.*, 2016, **311**, 75–84.
16 S. Royo, R. Martinez-Mañez, F. Sancenón, A. M. Cosetro, M. Parra and S. Gill, *Chem. Commun.*, 2007, 4839–4847.
17 L. Chen, D. Wu and J. Yoon, *ACS Sens.*, 2018, **3**, 27–43.
18 A. K. Das, S. Goswami, C. K. Quah and H. K. Fun, *RSC Adv.*, 2016, **6**, 18711–18717.
19 Y. J. Jang, O. G. Tsay, D. P. Murale, J. A. Jeong, A. Segev and D. G. Churchill, *Chem. Commun.*, 2014, **50**, 7531–7534.
20 V. Kumar, G. Raviraju, H. Rana, V. K. Rao and A. K. Gupta, *Chem. Commun.*, 2017, **53**, 1–4.
21 Y. Kim, Y. J. Jang, S. V. Mulay, T. T. T. Nguyen and D. G. Churchill, *Chem. – Eur. J.*, 2017, **23**, 7785–7790.
22 H. S. Sarkar, A. Ghosh, S. Das, P. K. Maiti, S. Maitra, S. Mandal and P. Sahoo, *Sci. Rep.*, 2018, **8**, 3402–3408.
23 BBC News - Enquiry into spray cancer claims. 2005-12-07.
24 J. Pritchard, AP IMPACT: Wal-Mart pulls jewelry over cadmium – Yahoo! News. 2010.
25 J. Gelles, McDonald's Recalls Cadmium-Tainted Shrek Glasses – Made in NJ, Huffington Post, 2010.
26 K. R. Nambiar, *Lasers: Principles, Types and Applications.*, 2004, ISBN 978-81-224-1492-9.
27 J. Goel, K. Kadirvelu, C. Rajagopal and V. K. Garg, *Ind. Eng. Chem. Res.*, 2006, **45**, 6531–6537.
28 C. Wang, Y. Fang, S. Peng, D. Ma and J. Zhao, *Chem. Res. Toxicol.*, 1999, **12**, 331–334.
29 S. Lofts, D. Spurgeon and C. Svendsen, *Environ. Sci. Technol.*, 2005, **39**, 8533–8540.
30 A. Martelli, E. Rousselet, C. Dycke, A. Bouron and J.-M. Moulis, *Biochimie*, 2006, **88**, 1707–1719.
31 B. Arvidson, *Toxicology*, 1994, **88**, 1–14.
32 W. C. Prozialeck, J. R. Edwards and J. M. Woods, *Life Sci.*, 2006, **79**, 1493–1506.
33 N. Cerullia, L. Campanellab, R. Grossib, L. Politic, R. Scandurrac, S. Giovanni, F. Galloe, S. Damianie, A. Alimontif, F. Petruccif and S. Caroli, *J. Trace Elem. Med. Biol.*, 2006, **20**, 171–179.
34 Q. D. Tuan and J. S. Kim, *Chem. Rev.*, 2010, **110**, 6280–6301.
35 G. Jiang, L. Xu, S. Song, C. Zhu, Q. Wu, L. Zhang and L. Wu, *Toxicology*, 2008, **244**, 49–55.
36 M. Waisberg, P. Joseph, B. Hale and D. Beyersmann, *Toxicology*, 2003, **192**, 95–117.
37 L. Järup and A. Åkesson, *Toxicol. Appl. Pharmacol.*, 2009, **238**, 201–208.
38 E. Marettováa, M. Maretta and J. Legáth, *Anim. Reprod. Sci.*, 2015, **155**, 1–10.
39 Beryllium, cadmium, mercury and exposures in the glass manufacturing industry. (IARC) International Agency for Research on Cancer, 1993, 58, IARC, Lyon, France, 119238.
40 IPCS (International Programme on Chemical Safety) Cadmium–Environmental Health Criteria 134, Geneva: World Health Organization; 1992. accessed 29 December 2009.
41 ATSDR Toxicological Profile for Cadmium, Agency for Toxic Substances and Disease Registry U.S. Department of Health and Human Services, Atlanta, GA, 2012.
42 World Health Organization, Avenue Appia 20, 1211 Geneva 27, Switzerland http://www.who.int/water_sanitation_health/dwq/chemicals/cadmium/en/.
43 M. J. Frisch, G. W. Trucks, H. B. Schlegel, G. E. Scuseria, M. A. Robb, J. R. Cheeseman, G. Scalmani, V. Barone, B. Mennucci, G. A. Petersson, H. Nakatsuji, M. Caricato, X. Li, H. P. Hratchian, A. F. Izmaylov, J. Bloino, G. Zheng, J. L. Sonnenberg, M. Hada, M. Ehara, K. Toyota, R. Fukuda, J. Hasegawa, M. Ishida, T. Nakajima, Y. Honda, O. Kitao, H. Nakai, T. Vreven, Jr., J. A. Montgomery, J. E. Peralta, F. Ogliaro, M. Bearpark, J. J. Heyd, E. Brothers, K. N. Kudin, V. N. Staroverov, R. Kobayashi, J. Normand, K. Raghavachari, A. Rendell, J. C. Burant, S. S. Iyengar, J. Tomasi, M. Cossi, N. Rega, J. M. Millam, M. Klene, J. E. Knox, J. B. Cross, V. Bakken, C. Adamo, J. Jaramillo, R. Gomperts, R. E. Stratmann, O. Yazyev, A. J. Austin, R. Cammi, C. Pomelli, J. W. Ochterski, R. L. Martin, K. Morokuma, V. G. Zakrzewski, G. A. Voth, P. Salvador, J. J. Dannenberg, S. Dapprich, A. D. Daniels, O. Farkas, J. B. Foresman, J. V. Ortiz, J. Cioslowskiand and D. J. Fox, *Gaussian 09, Revision A. 02*, Gaussian, Inc., Wallingford CT, 2009.